# Strong shock waves in a dense gas: Burnett theory versus Monte Carlo simulation

J. M. Montanero*
*Departamento de Electrónica e Ingeniería Electromecánica, Universidad de Extremadura, E-06071 Badajoz, Spain*

M. López de Haro†
*Centro de Investigación en Energía, Universidad Nacional Autónoma de México, Apartado Postal 34, Temixco, Morelos 62580, Mexico*

V. Garzó‡ and A. Santos§
*Departamento de Física, Universidad de Extremadura, E-06071 Badajoz, Spain*

(Received 20 February 1998)

Plane shock waves in a hard-sphere fluid are analyzed within the framework of the Enskog theory. The results are obtained from two different approaches: (i) the approximate solutions of the Enskog equation at the levels of the Navier-Stokes and the (linear) Burnett orders; and (ii) the exact solution of the Enskog equation obtained by means of a Monte Carlo simulation method. A comparison between the profiles of velocity, temperature, stress, and heat flux, as obtained from both approaches, is carried out. As expected, the shock becomes thinner (in units of the mean free path) as the density decreases and/or the Mach number increases. The approximate theoretical estimates for the shock thickness are smaller than the simulation values, but this discrepancy becomes less important as the density increases. In general, the linear Burnett theory is found to yield better results than the Navier-Stokes predictions, but both theories tend to overlap as the density increases, and, surprisingly enough, the Navier-Stokes estimates are even slightly superior to those of the linear Burnett theory at high Mach numbers. [S1063-651X(98)03012-8]

PACS number(s): 47.40.Nm, 47.50.+d, 05.20.Dd, 51.10.+y

## I. INTRODUCTION

One of the most interesting far from equilibrium states in a fluid is the one corresponding to a plane shock wave. It consists of a small, rapidly moving transition region in space connecting two equilibrium states, namely, a relatively cold, low-pressure region and a relatively hot, high-pressure region [1]. Under conditions of sufficiently high Mach number ($M \gtrsim 2$) in a dilute gas, it is a well-known fact that the shock profiles are not accurately described by the Navier-Stokes (NS) equations [2–6]. This has motivated the search for alternative theoretical approaches, such as the Burnett theory [3–7], the bimodal distribution of Mott-Smith [8], Grad's moment method [9], a modified NS theory [10], or a generalized hydrodynamics [11]. On the other hand, much less progress has been done in the case of dense fluids. Comparison between molecular dynamics simulations for a Lennard-Jones fluid and the NS profiles showed that the differences were relatively small [12,13]. In contrast, Frezzotti [14] has shown that, in the context of the Enskog equation, the NS theory is accurate only at low Mach numbers.

A natural question is whether, as happens in an ideal gas [3,4,6], the Burnett theory significantly improves over the NS theory when comparing with simulation or experimental data for dense gases. To our knowledge, this question has not been addressed in detail. This is mainly due to the fact that the density dependence of the transport coefficients is not explicitly known. A remarkable exception is the hard-sphere model, for which the Enskog theory provides a reliable description over a wide range of length and time scales [15]. In this framework, the Navier-Stokes coefficients [16] and the linear Burnett coefficients derived from the standard Enskog theory (SET) [17] and from the revised Enskog theory (RET) [18] are explicitly known as functions of density. Unfortunately, to our knowledge, the nonlinear Burnett coefficients, which are the same in both the SET and the RET [18], have not been derived so far.

The aim of this paper is to study shock waves for several values of density and the Mach number within the framework of the Enskog theory. This study will be carried out by means of two different but complementary routes: on the one hand, we will numerically solve both the NS and the linear Burnett hydrodynamic equations [19] by using the expressions for the corresponding transport coefficients derived from the Enskog equation; on the other hand, we will solve the full Enskog equation by means of a numerical algorithm. More specifically, we will use the recently proposed Enskog Simulation Monte Carlo (ESMC) method [20], which is an extension of the well-known direct simulation Monte Carlo (DSMC) method [21] to simulate the Boltzmann equation. Typically, as it also happens in the low-density case [3,4,6], the Burnett approximation represents a significant improvement over the NS approximation. However, this improvement is progressively less noticeable as the density increases, especially for high Mach numbers.

## II. HYDRODYNAMIC DESCRIPTION OF PLANE SHOCK WAVES

For plane shock waves it is convenient to choose a reference frame moving with the front, so that the shock is sta-

*Electronic address: jmm@unex.es
†Electronic address: malopez@servidor.dgsca.unam.mx
‡Electronic address: vicenteg@unex.es
§Electronic address: andres@unex.es

 

tionary in this frame. Under this condition, and taking the $x$ axis as the shock wave direction, the hydrodynamic balance equations yield

$$\rho(x)u(x)=\text{const}, \tag{1}$$

$$P_{xx}(x)+\rho(x)u^2(x)=\text{const}, \tag{2}$$

$$\rho(x)u(x)[e(x)+\tfrac{1}{2}u^2(x)]+P_{xx}u(x)+q(x)=\text{const}, \tag{3}$$

where $\rho$ is the mass density, $u$ is the $x$ component of the flow velocity, $P_{xx}$ is the relevant element of the pressure tensor, $e$ is the internal energy per mass unit, and $q$ is the $x$ component of the heat flux. Asymptotically far from the shock front, the fluid is at equilibrium, so that $q=0$ and $P_{xx}=p$, $p$ being the hydrostatic pressure. This leads to the well-known Rankine-Hugoniot conditions [1]

$$\rho_0 u_0=\rho_1 u_1, \tag{4}$$

$$p_0+\rho_0 u_0^2=p_1+\rho_1 u_1^2, \tag{5}$$

$$\rho_0 u_0(e_0+\tfrac{1}{2}u_0^2)+p_0u_0=\rho_1u_1(e_1+\tfrac{1}{2}u_1^2)+p_1u_1, \tag{6}$$

where hereafter the subscript 0 refers to quantities corresponding to the unshocked ''cold'' equilibrium state ($x\to-\infty$, upstream), while the subscript 1 refers to the shocked ''hot'' equilibrium state ($x\to\infty$, downstream).

Thus far, all the above equations apply to any fluid system. In order to close the problem we need to specify the relationship between the fluxes and the hydrodynamic gradients. To linear Burnett order and for the particular geometry of the problem, the constitutive equations can be written as

$$P_{xx}(x)=p(x)-[\tfrac{4}{3}\mu(x)+\kappa(x)]u'(x)-[\tfrac{4}{3}\alpha_3(x)-\alpha_1(x)]\rho''(x)+[\tfrac{2}{3}\alpha_4(x)+\alpha_2(x)]T''(x), \tag{7}$$

$$q(x)=-\lambda(x)T'(x)+[\tfrac{2}{3}\beta_1(x)-\beta_2(x)]u''(x), \tag{8}$$

where $p(x)$ is the local equilibrium pressure, $T(x)$ is the local temperature, and the primes denote spatial derivatives. The transport coefficients $\mu$ (shear viscosity), $\kappa$ (bulk viscosity), $\lambda$ (thermal conductivity), $\alpha_i$, and $\beta_i$ depend on space through their dependence on the local density and temperature. From Eq. (1) one easily has $\rho''=-\rho u''/u+2\rho u'^2/u^2$, so that, by consistency, we neglect the nonlinear term and replace in Eq. (7) $\rho''\to-\rho u''/u$. When the terms containing the second derivatives are dropped, one obtains the NS constitutive relations. In general, the explicit expressions of the transport coefficients are not known.

The above difficulties are partially overcome by choosing a hard-sphere system. In this case, the internal energy is simply proportional to the temperature, namely, $e=3k_BT/2m$ (where $k_B$ is the Boltzmann constant and $m$ is the mass of a particle), and the pressure is given by

$$p=\frac{\rho k_B T}{m}[1+4\eta\chi(\eta)], \tag{9}$$

where $\eta\equiv\pi\rho\sigma^3/6m$ is the packing fraction, $\sigma$ being the sphere diameter, and $\chi(\eta)$ is the equilibrium value of the pair correlation function at the point of contact. Here we will use the Carnahan-Starling approximation [22], i.e., $\chi(\eta)=(1-\eta/2)/(1-\eta)^3$. In addition, the Chapman-Enskog method [16] applied to the Enskog equation provides the density and temperature dependence of the transport coefficients. The NS coefficients can be found, for instance, in Ref. [16], while the linear Burnett coefficients given by the SET and the RET can be found in Refs. [17] and [18], respectively. When one inserts all these expressions into Eqs. (7) and (8), the balance equations (1)–(3) constitute a closed set of nonlinear differential equations for the unknowns $\rho(x)$, $u(x)$, and $T(x)$, subjected to the boundary conditions (4)–(6). Its solution must be carried out numerically. Due to the directional character of the mathematical stability of this set, the numerical integration has to start at the hot end, as first shown by von Mises [23] in the context of the NS equations. For more details about the numerical method employed in this paper, we refer the reader to Ref. [19].

In the plane shock wave problem it is convenient to scale the distance $x$ with the mean free path $\lambda_0=[\sqrt{2}\pi n_0\chi(\eta_0)\sigma^2]^{-1}$ of the hard-sphere gas in the cold region. Also, we choose the origin $x=0$ of the shock front as the point where $u=(u_0+u_1)/2$. The relevant dimensionless parameters characterizing the problem can be taken as the packing fraction $\eta_0$ upstream and the Mach number $M\equiv u_0/a_0$, where $a_0$ is the speed of sound upstream. By using well-known thermodynamics relations [24], the speed of sound $a$ of a hard-sphere fluid is

$$a=\left(\frac{5k_BT}{3m}\right)^{1/2}\left[1+8\eta\chi+\frac{4}{5}\eta^2(8\chi^2+3\chi')\right]^{1/2}, \tag{10}$$

where $\chi'\equiv d\chi/d\eta$. It must be emphasized that, for consistency, both $\lambda_0$ and $a_0$ refer to quantities of a *dense* gas. The latter point is especially important in order to interpret $M$ as the real Mach number, so that the shock wave only appears if $M>1$. This is in contrast to other choices, such as the ratio between $u_0$ and the speed of sound of an ideal gas [25].

## III. MONTE CARLO SIMULATION OF THE ENSKOG EQUATION

As is well known, a very fruitful and efficient algorithm to solve the Boltzmann equation is Bird's DSMC method [21]. In the context of a dense hard-sphere gas described by the Enskog equation, an extension of the DSMC method has been recently proposed [20]. This method has been shown to reproduce well the density dependence of the Enskog transport coefficients, namely, the shear viscosity [20], the viscometric functions [26], and the thermal conductivity [27]. As applied to the plane shock wave problem, the ESMC method proceeds as follows. A system of length $D$ along the $x$ direction is occupied by a sufficiently high number $N$ of particles. The boundaries of the system must be sufficiently far away from the shock front, so that they can be considered to be at equilibrium. This implies that $D$ is much larger than the shock thickness $\delta$. The system is split into $L$ layers of width $\Delta x=D/L$ smaller than $\delta$. The *physical* density of layer $I=1,\ldots,L$ is $n_I=\overline{n}L(N_I/N)$, where $\overline{n}$ is the average density and $N_I$ is the number of *simulated* particles in cell $I$. Those particles lying in cells separated from the boundaries a dis-

tance smaller than or equal to $\sigma$ represent ''bath'' particles, while the remaining ones represent ''actual'' particles. The role of bath particles is to sample the conditions in the upstream and downstream domains, so that their velocity distributions are kept to be Maxwellians. At integer times $t=\Delta t,2\Delta t,3\Delta t,\ldots$, the positions $\{x_i\}$ and velocities $\{\mathbf{v}_i\}$ are updated due to free streaming and collisions. In the free-streaming stage, $x_i\to x_i+v_{ix}\Delta t$; if a particle leaves the system, it is reentered through the opposite boundary with the same velocity, so that the mass flux is constant [Eq. (1)]. Before proceeding to the collision stage, the velocities of the bath particles are replaced by random velocities selected from the corresponding equilibrium probability distributions characterized by the upstream or downstream hydrodynamic quantities, namely, $u_{0,1}$ and $T_{0,1}$ [6].

The essential distinction between the DSMC and ESMC methods appears in the collision stage, in parallel to what happens between the Boltzmann and Enskog equations [16]. For each cell $I$ a sample of $\frac{1}{2}N_I\omega_{\max}$ particles are randomly chosen with equal probability, where $\omega_{\max}$ is an upper bound of the quantity $\omega_{ij}$ defined below. For each particle $i$ belonging to this sample, the following steps are taken: (1) a given direction $\hat{\boldsymbol{\sigma}}_i$ is chosen at random with equiprobability, and the layer $J$ containing the point $x_i+\sigma\hat{\sigma}_{ix}$ is identified; (2) a particle $j$ belonging to layer $J$ is selected at random; (3) the collision between particles $i$ and $j$ is accepted with a probability equal to $\Theta(\hat{\boldsymbol{\sigma}}_i\cdot\mathbf{g}_{ij})\omega_{ij}/\omega_{\max}$, where $\mathbf{g}_{ij}\equiv\mathbf{v}_i-\mathbf{v}_j$ and $\omega_{ij}\equiv\sigma^2 4\pi(\hat{\boldsymbol{\sigma}}_i\cdot\mathbf{g}_{ij})\chi_{ij}n_J\Delta t$, $\chi_{ij}$ being the pair correlation associated with the positions of the spheres $i$ and $j$; and (4) if the collision is accepted, the post-collision velocities are assigned, namely, $\mathbf{v}_i\to\mathbf{v}_i-(\hat{\boldsymbol{\sigma}}_i\cdot\mathbf{g}_{ij})\hat{\boldsymbol{\sigma}}_i$, $\mathbf{v}_j\to\mathbf{v}_j+(\hat{\boldsymbol{\sigma}}_i\cdot\mathbf{g}_{ij})\hat{\boldsymbol{\sigma}}_i$, except if $i$ and/or $j$ is a bath particle, in which case its velocity is unchanged. In our simulations we have implemented the SET rather than the RET. This implies that $\chi_{ij}=\chi(\eta_K)$, where $K$ denotes the layer equidistant from layers $I$ and $J$. In order to avoid any systematic bias, the sorting of the cells $I$ is chosen randomly.

The values of the technical parameters $D$, $N$, $\Delta x$, and $\Delta t$ have been chosen depending on the case considered. For example, in the case where $\eta_0=0.2$ and $M=1.3$ we have taken $D=70\lambda_0$, $N=350\,000$, $\Delta x=0.1\lambda_0$, and $\Delta t=0.003\lambda_0/\sqrt{2k_BT_0/m}$. As the shock front becomes sharper (as $\eta_0$ decreases and/or $M$ increases), the values of $\Delta x$ and $\Delta t$ must be chosen smaller. To shorten the transient time, the initial condition has been taken as corresponding to two different equilibrium distributions for $x<0$ and $x>0$. Once a steady state is reached, the hydrodynamic profiles are measured as time averages and also as averages over 5–10 independent realizations.

## IV. RESULTS

As a first case, we consider $\eta_0=0.2$ and $M=1.3$. Figure 1 shows the velocity and temperature profiles as obtained from the simulations and from the NS approximation. As expected, since the Mach number has a moderate value, the NS equations describe the shock profiles accurately. In these conditions, the shock thickness is $\delta\sim 30\lambda_0$. We have also compared our Monte Carlo data with those obtained by Frezzotti [28] from a numerical solution of the Enskog equation and from molecular dynamics simulations, and we have found an excellent agreement. This confirms that the SET provides a reliable theory for this relatively dense shock wave.

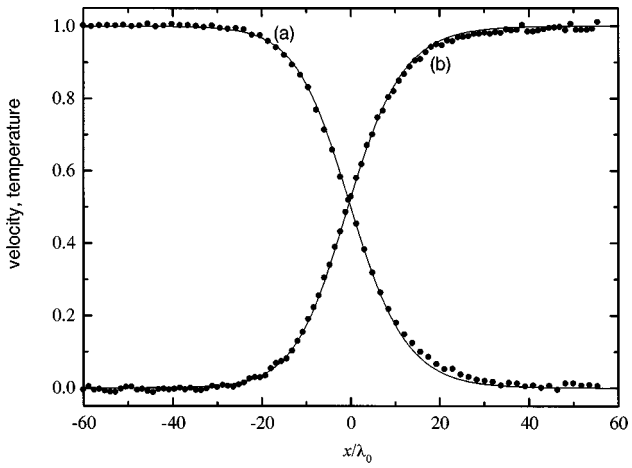


FIG. 1. Profiles of (a) the reduced velocity $(u-u_1)/(u_0-u_1)$ and (b) the reduced temperature $(T-T_0)/(T_1-T_0)$ at $\eta_0=0.2$ and $M=1.3$. The solid lines refer to the Navier-Stokes solution, and the circles correspond to the simulation data.

Discrepancies between the NS profiles and the simulation ones appear when one considers larger Mach numbers or smaller densities. As an illustration, Fig. 2 shows the velocity and temperature profiles for $\eta_0=0.1$ and $M=2$, now including the predictions obtained from the linear Burnett approximation with transport coefficients given by the Enskog theory. In the latter case we have considered both the SET and RET, but the respective profiles are practically indistinguishable. The Burnett profiles are interrupted on the cold side of the front due to the numerical instability of the numerical solution [19]. This does not represent a serious drawback, since the cold side is well described by the NS theory and the same is expected to hold for the Burnett theory. In addition, this instability does not affect the evaluation of the shock thickness (see below), as the hydrodynamic quantities

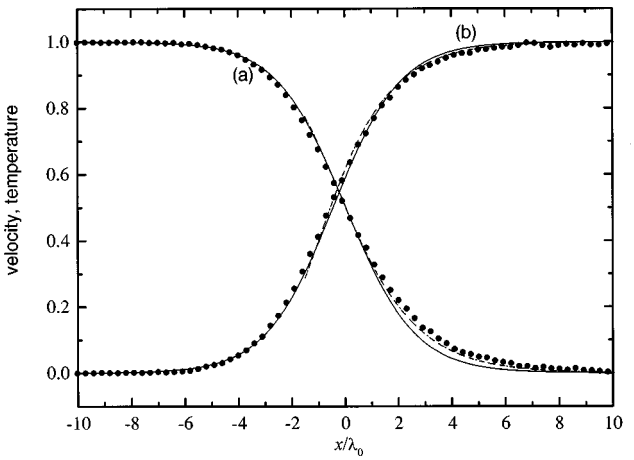


FIG. 2. Profiles of (a) the reduced velocity $(u-u_1)/(u_0-u_1)$ and (b) the reduced temperature $(T-T_0)/(T_1-T_0)$ at $\eta_0=0.1$ and $M=2$. The solid and dashed lines refer to the Navier-Stokes and Burnett solutions, respectively, and the circles correspond to the simulation data.

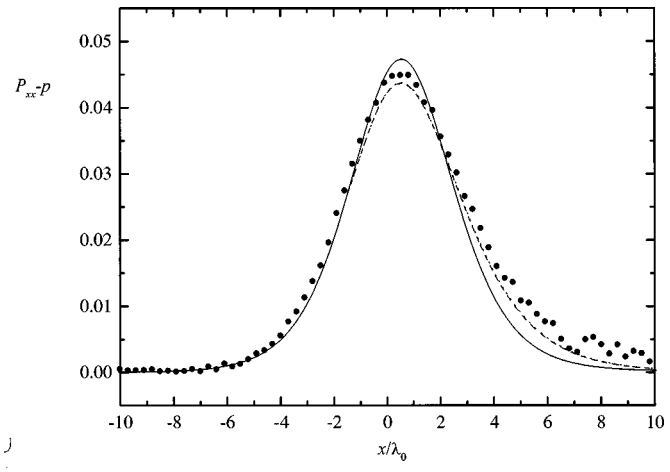


FIG. 3. The same as in Fig. 2, but for the stress $P_{xx}-p$, measured in units of $2k_BT_0/\lambda_0^3$.

near their inflection points are rather stable. On the other hand, Fiscko and Chapman [3] were able to overcome this difficulty in the case of a dilute gas by solving the time-dependent equations rather than the steady-state ones. From Fig. 2 we observe that the (linear) Burnett correction significantly improves the agreement with the simulation data on the hot side of the front, as well as the shock thickness ($\delta \sim 6\lambda_0$). The improvement of the Burnett theory over the NS theory is even more noticeable in Figs. 3 and 4, where the profiles of the stress $P_{xx}-p$ and the heat flux $q$ are plotted.

In order to carry out a more systematic study, it is convenient to introduce a parameter characterizing the thickness of the shock front. As usual [3,4,11,21,25], we define the reciprocal shock thickness as the maximum value of the normalized density gradient:

$$\delta^{-1}=\frac{1}{n_1-n_0}\left(\frac{dn}{dx}\right)_{\max}. \tag{11}$$

The density dependence of $\delta^{-1}$ at $M=2$ is shown in Fig. 5. Both the NS and linear Burnett theories correctly predict that the shock thickness (in units of the upstream mean free path) increases with density. On the other hand, both theories lead

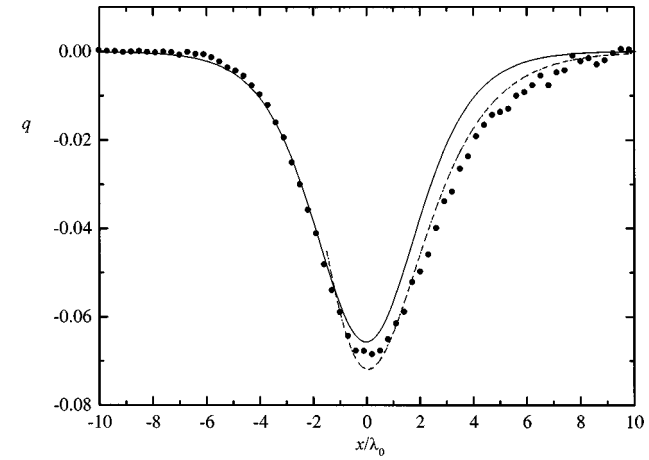


FIG. 4. The same as in Fig. 2, but for the heat flux $q$, measured in units of $m(2k_BT_0/m)^{3/2}/\lambda_0^3$.

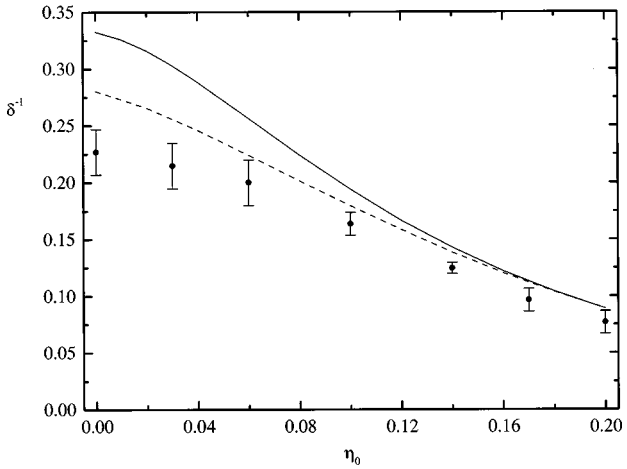


FIG. 5. Density dependence of the reciprocal shock thickness (in units of the mean free path $\lambda_0$) at $M=2$. The solid and dashed lines correspond to the Navier-Stokes and Burnett solutions, respectively, while the circles are simulation results.

to shock fronts thinner than the correct ones. While, in general, the Burnett estimate is better than the NS one, the (linear) Burnett correction becomes less important as the density increases. At $\eta_0=0$ the NS and Burnett deviations from the simulation value of $\delta$ are about 32% and 19%, respectively, while at $\eta_0=0.2$ both theories give practically the same deviation of about 14%. The monotonic increase of $\delta/\lambda_0$ with $\eta_0$ contrasts with previous results [25], where a nonmonotonic behavior was claimed. It is also interesting to note that, when measured in units of the sphere diameter $\sigma$, the shock thickness decreases as the density increases, at least in the density range considered. At $M=2$, for instance, $\delta/\sigma$ is infinite in the limit $\eta_0\to 0$, it is equal to 5.5 at $\eta_0=0.1$, and it takes the value 4.4 at $\eta_0=0.2$.

As a complement, the dependence of $\delta$ on $M$ for several values of the density is displayed in Fig. 6. As the Mach number decreases the shock thickness increases, becoming infinite in the limit $M\to 1$. The monotonic behavior of $\delta/\lambda_0$

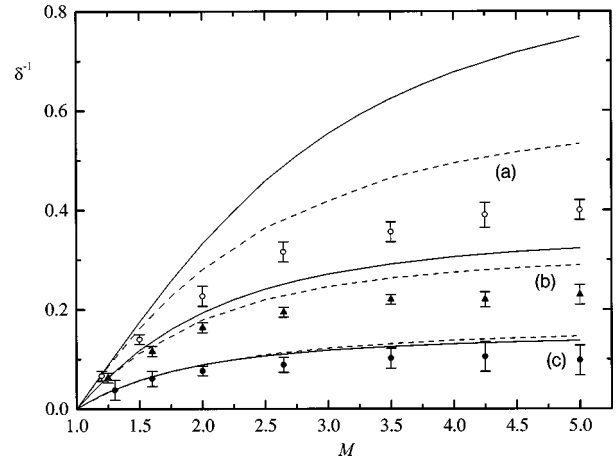


FIG. 6. Plot of the reciprocal shock thickness (in units of the mean free path $\lambda_0$) as a function of the Mach number at (a) $\eta_0=0$, (b) $\eta_0=0.1$, and (c) $\eta_0=0.2$. The solid and dashed lines correspond to the Navier-Stokes and Burnett solutions, respectively, while the symbols are simulation results.

as a function of $\eta_0$ observed in Fig. 5 at $M=2$ is confirmed in Fig. 6 for the range $1<M<5$. In general, we see again an improvement of the linear Burnett predictions over those from the NS theory, except at the highest density considered ($\eta_0=0.2$), where, surprisingly, the Burnett thickness is smaller than the NS thickness for sufficiently large Mach numbers. This could be due to the absence of nonlinear Burnett terms in the constitutive equations or to the nonconvergent asymptotic character of the Chapman-Enskog expansion [29]. It must be noted that, in the case of a low-density gas of particles interacting with a potential softer than that of hard spheres, there exists a value $M^*$ of the Mach number for which $\delta$ reaches a minimum, so that $\delta$ increases for $M>M^*$ [3,4,11,21]. For instance, $M^*\simeq 3$ for Maxwell molecules. However, in the case of a dilute gas of hard spheres, $\delta$ increases with $M$ and tends to a given value, at least according to the NS theory [21]. Our results for $\eta_0=0$ support this conclusion. The results plotted in Fig. 6 for $\eta_0=0.1$ and 0.2 seem to indicate that either the asymptotic value of $\delta$ is practically reached for smaller values of $M$ than in the low-density gas, or that there also exists a maximum value at a certain $M^*(\eta_0)$.

## V. DISCUSSION

In this paper we have addressed the problem of plane shock waves in a dense hard-sphere gas within the framework of the Enskog theory. The results have been obtained from two different routes: (i) the numerical solution of the hydrodynamic equations in the NS order and in the (linear) Burnett order with transport coefficients given by the Enskog theory, and (ii) the Monte Carlo simulation of the Enskog equation. We have considered a range $0\leqslant\eta_0\leqslant 0.2$ for the packing fraction of the fluid in the cold (upstream) region and a range $1\leqslant M\leqslant 5$ for the Mach number. The results indicate that the theoretical predictions underestimate the shock thickness $\delta$, this effect becoming more important as $\delta/\lambda_0$ decreases (i.e., at low densities and high Mach numbers). In general, the linear Burnett theory presents a better agreement with the simulation data than the NS theory. However, the estimates of both theories become closer as the density increases, and even the Burnett corrections are slightly worse than the NS estimates at high Mach numbers. This latter fact could be due to the absence in the theory of nonlinear Burnett terms, which so far are not explicitly known for a dense hard-sphere gas. In the low-density limit, however, the influence of the nonlinear Burnett terms is relatively small; at $M=5$, for instance, the value of the reciprocal thickness $\delta^{-1}$ as obtained from the linear (nonlinear) Burnett theory is 0.71 (0.72) times the NS value and 1.33 (1.35) times the simulation value. In this respect it is interesting to remark that Chapman and co-workers [3–5] found that the addition of third order (super-Burnett) terms to the Burnett equations only slightly affects the shock structure. Whether this small influence on the linear Burnett solution of nonlinear Burnett terms and linear and nonlinear super-Burnett terms also holds for finite densities is of course uncertain. Another possible explanation could be related to the asymptotic character of the Chapman-Enskog expansion.

As a general conclusion, we remark that the NS theory provides a better description of plane shock waves for dense gases than for dilute gases, thus confirming previous observations [12,13]. This is related to the fact that, although the shock becomes thinner in real units (e.g., in units of $\sigma$) as the density increases, the thickness increases when expressed in units of the mean free path. For small nonzero densities the (linear) Burnett theory improves over the NS description, but for moderate and/or large densities the (linear) Burnett theory is not enough, so that other approaches should be considered. An alternative approach could be the extension of Grad's moment method to the case of the Enskog equation which was recently applied to the uniform shear flow [30].

Finally, it is worth pointing out that, since the results have been derived from the Enskog description for a dense hard-sphere fluid, the above conclusions cannot be extrapolated without caution to real systems. Nevertheless, here we have restricted ourselves to the regime of moderate densities ($\eta_0\leqslant 0.2$), where the NS transport coefficients given by the Enskog theory are known to agree well with molecular dynamics results [31]. In addition, the shock profiles obtained from the Enskog equation for $\eta_0=0.2$ and $M=1.3$ show a good agreement with those given by molecular dynamics simulations [28]. It remains an open question for the future, whose answer may hopefully be motivated by our results, to check whether this agreement extends to higher values of the Mach number.

## ACKNOWLEDGMENTS

We are grateful to Aldo Frezzotti for providing us data from his numerical solution of the Enskog equation. This research was supported by the DGES (Spain) through Grant No. PB97-1501, and by the Junta de Extremadura (Fondo Social Europeo) through Grant No. PRI97C1041.

[1] J. O. Hirschfelder, C. F. Curtiss, and R. B. Bird, *Molecular Theory of Gases and Liquids* (Wiley, New York, 1954).

[2] H. W. Liepmann, R. Narashima, and M. T. Chahine, Phys. Fluids **5**, 1313 (1962).

[3] K. A. Fiscko and D. R. Chapman, in *Rarefied Gas Dynamics*, edited by E. P. Muntz, D. P. Weaver, and D. H. Campbell, Progress in Astronautics and Aeronautics Vol. 118 (AIAA, Washington, DC, 1989), pp. 374–395. This is the first paper where evidence is presented about the improvement of the Burnett relative to the Navier-Stokes equations for dilute gases. However, the quantitative results of this paper have some inaccuracies that are corrected in Ref. [4].

[4] F. E. Lumpkin III and D. R. Chapman, J. Thermophys. Heat Transfer **6**, 419 (1992).

[5] X. Zhong, R. W. MacCormack, and D. R. Chapman, AIAA J. **31**, 1036 (1993).

[6] E. Salomons and M. Mareschal, Phys. Rev. Lett. **69**, 269 (1992).

[7] C. S. Wang Chang, in *Studies in Statistical Mechanics V*, edited by J. de Boer and G. E. Uhlenbeck (North-Holland, Am-

sterdam, 1970), pp. 27–42.
[8] H. M. Mott-Smith, Phys. Rev. **82**, 885 (1951).
[9] H. Grad, Commun. Pure Appl. Math. **5**, 257 (1952); L. H. Holway, Phys. Fluids **7**, 911 (1964); W. Weiss, Phys. Rev. E **52**, R5760 (1995); Phys. Fluids **8**, 1689 (1996).
[10] B. L. Holian, Phys. Rev. A **37**, 2562 (1988); B. L. Holian, C. W. Patterson, M. Mareschal, and E. Salomons, Phys. Rev. E **47**, R24 (1993).
[11] M. Al-Ghoul and B. C. Eu, Phys. Rev. E **56**, 2981 (1997).
[12] W. G. Hoover, Phys. Rev. Lett. **42**, 1531 (1979).
[13] B. L. Holian, W. G. Hoover, B. Moran, and G. K. Straub, Phys. Rev. A **22**, 2798 (1980).
[14] A. Frezzotti, in *Rarefied Gas Dynamics 19*, edited by J. Harvey and G. Lord (Oxford University Press, Oxford, 1995), pp. 455–461.
[15] H. van Beijeren and M. H. Ernst, Phys. Lett. A **43**, 637 (1973); Physica A **68**, 437 (1973).
[16] J. Ferziger and H. Kaper, *Mathematical Theory of Transport Processes in Gases* (North-Holland, Amsterdam, 1972).
[17] S. R. Alves and G. Kremer, Physica A **164**, 759 (1990).
[18] M. López de Haro and V. Garzó, Physica A **197**, 98 (1993).
[19] M. López de Haro and V. Garzó, Phys. Rev. E **52**, 5688 (1995).
[20] J. M. Montanero and A. Santos, Phys. Rev. E **54**, 438 (1996); Phys. Fluids **9**, 2057 (1997); see also A. Frezzotti, *ibid.* **9**, 1329 (1997).
[21] G. A. Bird, *Molecular Gas Dynamics and the Direct Simulation of Gas Flows* (Clarendon, Oxford, 1994).
[22] N. F. Carnahan and K. E. Starling, J. Chem. Phys. **51**, 635 (1969).
[23] R. von Mises, J. Aeronaut. Sci. **17**, 551 (1950).
[24] H. B. Callen, *Thermodynamics* (Wiley, New York, 1959).
[25] A. Frezzotti and C. Sgarra, J. Stat. Phys. **73**, 193 (1993).
[26] J. M. Montanero and A. Santos, Physica A **240**, 229 (1997).
[27] J. M. Montanero and A. Santos, in *Rarefied Gas Dynamics 20*, edited by C. Shen (Peking University Press, Beijing, 1997), pp. 137–142.
[28] A. Frezzotti, Physica A **240**, 202 (1997); Comput. Math. Appl. **35**, 103 (1998). Notice that the case $\eta_0=0.2$, $M=1.3$ corresponds, in Frezzotti's notation, to a piston speed $V_p=2.582(k_BT_0/m)^{1/2}$.
[29] H. Grad, Phys. Fluids **6**, 147 (1963); J. A. McLennan, *ibid.* **8**, 1580 (1965); G. Scharf, Helv. Phys. Acta **40**, 929 (1967); A. Santos, J. J. Brey, and J. W. Dufty, Phys. Rev. Lett. **56**, 1571 (1986).
[30] J. F. Lutsko, Phys. Rev. Lett. **78**, 243 (1997); Phys. Rev. E **58**, 434 (1998).
[31] J. R. Dorfman and H. van Beijeren, in *Statistical Mechanics. Part B: Time-Dependent Processes*, edited B. J. Berne (Plenum, New York, 1977), pp. 65–179.